

Rhodopsin-Interacting Surface of the Transducin  $\gamma$  Subunit<sup>†</sup>Oleg G. Kisselev<sup>\*,‡,§</sup> and Maureen A. Downs<sup>‡</sup>*Departments of Ophthalmology and of Biochemistry and Molecular Biology, Saint Louis University School of Medicine, St. Louis, Missouri 63104**Received April 25, 2006; Revised Manuscript Received June 7, 2006*

**ABSTRACT:** The visual signaling pathway is initiated by photoactivation of the GPCR rhodopsin, which activates nucleotide exchange on the heterotrimeric G-protein transducin (Gt). Domains on both Gt $\alpha$  and Gt $\beta\gamma$  subunits participate in coupling to rhodopsin. Previously, we have shown by high-resolution NMR that the farnesylated C-terminal peptide of Gt $\gamma$ (60–71), DKNPFKELKGGC, assumes an amphipathic helical conformation during interaction with metarhodopsin II [Kisselev, O. G., and Downs, M. A. (2003) *Structure* 11, 367–373]. This conformation was docked to the structure of holo-Gt to create a model of rhodopsin–Gt interaction. Here we test this model by mutational analysis of Gt. To evaluate the contribution of specific amino acids of the Gt $\gamma$  C-terminal region involved in binding and GTP-dependent release of transducin from native rhodopsin membranes, we have systematically substituted each of the amino acids in the C-terminal region of Gt $\gamma$  for alanine. The mutants were co-expressed with six-histidine-tagged Gt $\beta\gamma$  subunits in Sf9 insect cells. The Gt $\beta$ -6-His- $\gamma$  mutant proteins were purified and assayed in the presence of Gt $\alpha$  for the GTP-dependent interactions with light-activated rhodopsin. Several of the alanine mutants, N62A, P63A, and F64A, exhibited significant functional defects at the level of R\*–Gt complex formation. These data show that the conserved N-terminal end of the helical domain in the Gt $\gamma$ (60–71) region has the most significant effect on rhodopsin–Gt interactions, which places important constraints on the model of the rhodopsin–Gt complex.

Transducin is a retinal rod cell specific heterotrimeric GTP-binding protein, or G-protein, responsible for transducing visual signals from rhodopsin to the cGMP phosphodiesterase (1–3). The GTP-bound transducin  $\alpha$  subunit, Gt $\alpha$ -GTP, is a molecular switch ultimately responsible for activating the effector enzyme. The initial interaction with the light-activated rhodopsin, R\*, and nucleotide exchange on Gt $\alpha$  are dependent on the tight  $\beta\gamma$  subunit complex, Gt $\beta\gamma$ . Both the GDP-bound transducin  $\alpha$  subunit, Gt $\alpha$ -GDP, and Gt $\beta\gamma$  have specialized protein domains involved in R\* interactions. The carboxyl-terminal region of Gt $\gamma$ , which is modified posttranslationally by farnesylation and carboxymethylation, is the primary domain of Gt $\beta\gamma$  involved in R\*–Gt $\beta\gamma$  interactions (4).

Recent NMR studies of a synthetic peptide, Gt $\gamma$ (60–71)-farnesyl, bound to R\* (5) and photoaffinity labeling studies using holotransducin (6) show that the C-terminal region of Gt $\gamma$  is involved in conformational rearrangements that change the position of both the amino acid residues of Gt $\gamma$ (60–71) and the farnesyl moiety during binding to R\*. These results support conclusions made earlier about unmasking of the Gt $\gamma$  C-terminal domain upon binding of Gt to R\*, based on

the specific antibody recognition and Gt $\gamma$  tail accessibility to the carboxypeptidase Y (7). The NMR study proposed that Gt $\gamma$ (60–71) assumes an amphipathic helical conformation upon binding to R\*. A molecular model of the R\*–Gt complex was on the basis of the computer docking of the peptide structure to the Gt structure in the inactive state. To test this model on the level of holo-Gt, for detailed understanding of the R\*–Gt interaction mechanism, and to elucidate the contribution of individual residues of Gt $\gamma$  in R\* binding, we replaced each individual amino acid in the Gt $\gamma$ (60–71) region with alanine. Recombinant Gt $\beta\gamma$  mutants were expressed in an insect cell/baculovirus expression system, purified, and reconstituted with purified retinal Gt $\alpha$ . The ability of mutant proteins to interact with R\* in the native lipid membrane was assessed by a Gt binding and GTP-dependent release assay. The results identify the molecular surface of Gt $\gamma$  involved in R\* interactions, which is important for building a model of the R\*–Gt complex.

**MATERIALS AND METHODS**

*Insect Cells and Construction of Baculoviruses Containing Mutant Gt $\gamma$ .* *Spodoptera frugiperda* Sf9 cells were obtained from ATCC (ATCC CRL 1711) and maintained in suspension at 27 °C at 120 rpm in Sf-900 II SFM medium (Gibco BRL) or in Grace's complete. Erlenmeyer flasks with the cell suspension were shaken in an INNOVA model 4000 device (New Brunswick Scientific) equipped with a refrigeration unit to maintain a temperature of 27 °C. Cells were kept between  $1 \times 10^6$  and  $3 \times 10^6$  cells/mL in the log phase. Gt $\gamma$ 1 (bovine) mutants were constructed using PCR by introducing desired nucleic acid substitutions into the 3'

<sup>†</sup> Supported in part by Research to Prevent Blindness, the Norman J. Stupp Foundation, the American Heart Association, and NIH Grant GM63203.

\* To whom correspondence should be addressed: Departments of Ophthalmology and of Biochemistry and Molecular Biology, Saint Louis University School of Medicine, 1755 South Grand Blvd., St. Louis, MO 63104. Phone: (314) 256-3253. Fax: (314) 771-0596. E-mail: kisselev@slu.edu.

<sup>‡</sup> Department of Ophthalmology.

<sup>§</sup> Department of Biochemistry and Molecular Biology.

primer, which also had an XbaI restriction site introduced immediately after the TAA stop codon for easy subcloning. The 5' primer contained the engineered PstI site but was otherwise identical to the wild-type nucleic acid sequence in the untranslated region of Gt $\gamma$  immediately preceding the ATG start codon. The baculoviruses were constructed using the Bac-to-Bac Baculovirus Expression System (Gibco BRL). The mutant cDNA was subcloned into the pFastBac vector (Invitrogen) for transformation of DH5- $\alpha$  competent cells (Gibco). Transformants were grown on LB-ampicillin plates for selection. The DNA from positive colonies was isolated using the Wizard miniprep kit (Promega) and analyzed by digestion with appropriate restriction endonucleases and DNA sequencing.

For transposition into the bacmid, pFastBac/ $\gamma$ 1 mutant DNA was added to DH10Bac competent cells (Invitrogen) on ice and incubated for 30 min, heat shocked at 42 °C for 45 s, and placed on ice; 300  $\mu$ L of SOC medium was added and then the mixture incubated in a 37 °C shaker for 4 h. Serial dilutions of transposition mix in SOC medium were prepared, and 100  $\mu$ L of undiluted and serially diluted mix was plated onto Luria agar plates containing 50  $\mu$ g/mL kanamycin, 7  $\mu$ g/mL gentamicin, 10  $\mu$ g/mL tetracycline, 100  $\mu$ g/mL Bluo-gal, and 40  $\mu$ g/mL IPTG and the mixture incubated for 48 h at 37 °C for color development. White colonies were restreaked on Luria agar complete plates and subcultured. Isolation of the recombinant bacmid and SF9 cell transformation were performed as per the Bac-to-Bac Baculovirus Expression System protocol using cellfectin. The nucleotide sequence of Gt $\gamma$  in each bacmid was confirmed by DNA sequencing. Each virus was amplified four times to produce a high-titer stock. His-tagged Gt $\beta$ 1 baculovirus was a gift from T. Kozasa.

**Protein Expression and Purification.** Purification of the recombinant Gt $\beta\gamma$  subunits was essentially as described previously (8). Prior to large-scale protein expression, the  $\beta$ 1: $\gamma$ 1 ratio was titrated to that of the native Gt $\beta\gamma$  complex by adjusting the ratios of the  $\beta$ 1 and  $\gamma$ 1 viruses and monitoring the protein expression by immunoblotting with antibodies against Gt $\gamma$ 1 and Gt $\beta$ 1 subunits on a Western blot (9). Large protein preparations were made in 500 mL cultures at a density of  $1 \times 10^6$  SF9 cells/mL in Grace's complete. On average, the protein production peaked 36–48 h post-infection. Infected cells were pelleted at 3000 rpm and 4 °C for 15 min, decanted and resuspended in 30 mL of ice-cold membrane wash buffer (MWB) [50 mM sodium phosphate (pH 8), 150 mM NaCl, 10 mM  $\beta$ -mercaptoethanol, 21  $\mu$ g/mL PMSF, 0.01% TLCK, and 0.01% TPCK], and lysed in Parr bomb on ice at 1000 psi for 30 min. The cell lysate was centrifuged at 310000g in a Beckman ultracentrifuge at 4 °C for 30 min, aspirated, and resuspended in 2 mL of MWB.

For membrane binding studies, aliquots of the pellet, which represented the membrane fraction, and aliquots of the supernatant, containing the cytosolic fraction, were saved for immunoblotting analysis. For protein purification, the pellet was homogenized with a Potter-Elvehjem homogenizer and the protein concentration was measured using a Bradford assay (Bio-Rad). The protein was solubilized with 1% octyl glucoside; the protein concentration was adjusted to 5 mg/mL, and the protein was incubated on ice for 1 h with frequent homogenizing and then pelleted in a 70Ti rotor at

310000g and 4 °C for 30 min. Proteins were affinity purified on a Ni–NTA agarose column (Qiagen). The purified Gt $\beta$ -6-His–Gt $\gamma$  protein complex was eluted per the Qiagen protocol, dialyzed in 10 mM Tris–HCl (pH 8), 150 NaCl, and 10 mM  $\beta$ -mercaptoethanol, concentrated, and stored in the presence of 50% glycerol at –20 °C. The purified protein was analyzed by silver staining (10) and immunoblotting. The concentration of all mutants was normalized to that of a recombinant wild type to ensure accurate comparison of activities in functional assays.

**Rod Outer Segment Preparation and Gt Purification.** Dark-adapted frozen bovine retinas were obtained from W. L. Lawson, Co. Rod outer segments (ROS) were prepared by the method of Papermaster and Dreyer as we described (9). Urea-washed ROS membranes (UM) were prepared using the procedure adapted from Yamazaki et al. (11) and Willardson et al. (12). The purity of rhodopsin was assessed by SDS–PAGE and protein staining with silver (10). The rhodopsin concentration was measured as  $\Delta A_{498}$  before and after bleaching in the presence of 20 mM hydroxylamine, based on the molar extinction coefficient at 498 nm of 42 700 M $^{-1}$  cm $^{-1}$ . ROS disk membranes were resuspended in ROS-Iso buffer [10 mM Tris–HCl (pH 7.4), 100 mM NaCl, 5 mM MgCl $_2$ , 1 mM DTT, and 0.1 mM PMSF] and stored at –70 °C.

Gt was purified by GTP elution from isotonicity washed ROS disks, and Gt $\alpha$  and Gt $\beta\gamma$  were separated by AKTA FPLC on Blue-Sepharose Cl-6B. ROS disks were resuspended under bright light in ROS-Hypo buffer for 10 min. The suspension was centrifuged at 250000g for 20 min (Ti-60, Beckman), and the pellet was washed in ROS-Hypo [10 mM Tris–HCl (pH 7.4), 0.5 mM MgCl $_2$ , 1 mM DTT, and 0.1 mM PMSF] by the same procedure once more. Gt was released by three additional washes with ROS-Hypo buffer and 100  $\mu$ M GTP. Supernatants of the GTP-containing washes were combined, and Gt $\alpha$  and Gt $\beta\gamma$  were separated by AKTA FPLC on a 25 mL Blue-Sepharose Cl-6B column (Pharmacia) equilibrated in 10 mM HEPES (pH 7.5), 5 mM MgSO $_4$ , 1 mM EDTA, 1 mM DTT, and 10  $\mu$ M PMSF. Gt is applied at a rate of 0.5 mL/min at 4 °C. Unbound fractions were collected and analyzed by SDS–PAGE, and those containing Gt $\beta\gamma$  were combined and concentrated to 1–2 mL on the mini DEAE-Sephacel column. After a short 20 mL wash, Gt $\alpha$  bound to the Blue-Sepharose was eluted with a 75 mL linear gradient of KCl (from 0 to 1 M) in a column equilibration buffer. Fractions containing Gt $\alpha$  were combined and concentrated to 1–2 mL by ultrafiltration using an Amicon PM-10 filter. Finally, Gt $\alpha$  and Gt $\beta\gamma$  were desalted separately on a Superose-12 gel filtration column by AKTA FPLC [flow rate of 1 mL/min; final buffer of 10 mM Tris–HCl (pH 7.5), 1 mM MgCl $_2$ , and 1 mM DTT]. Fractions were analyzed by SDS–PAGE and silver staining. Protein concentrations were determined by the Bio-Rad protein assay, using BSA as a standard. Separated subunits of transducin were aliquoted and stored at –20 °C in the presence of 50% glycerol.

**R\*–Gt Binding and Release Assay.** Various amounts of Gt $\beta\gamma$  (0, 0.1, 0.25, 0.4, 0.55, and 0.7  $\mu$ g) were reconstituted with 3  $\mu$ g of Gt $\alpha$  and 30  $\mu$ g of urea-washed ROS membranes (UM) in 100  $\mu$ L of buffer [10 mM Tris–HCl (pH 7.4), 100 mM NaCl, 5 mM MgCl $_2$ , 1 mM DTT, and 0.1 mM PMSF] under dark-red light on ice essentially as we described (9).

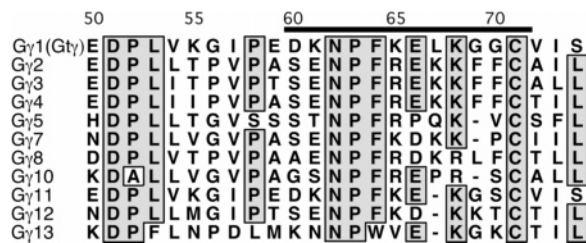


FIGURE 1: Amino acid sequence alignment of the Gtγ(50–71) region with the corresponding amino acid sequences of various subtypes of Gγ subunits. All Gγ subunits are mouse specific, except for Gtγ10 and Gtγ13 (human) and Gtγ12 (bovine). The black bar represents the region targeted by the alanine replacements.

In control reactions, the Gtα was omitted. An aliquot of the reaction mixture was taken at this stage to assess binding of Gt to dark-adapted rhodopsin membranes. This aliquot was centrifuged, and the pellet was washed twice with ROS-Iso buffer in the dark. The reaction was initiated by exposure of the rest of the samples to 480 nm light, followed by a 15 min incubation at 4 °C. UM were centrifuged at 109000g and 4 °C for 10 min in a TLA-100.3 rotor on a Beckman TL-100 ultracentrifuge. The pellet was washed twice with ROS-Iso buffer, and another aliquot was taken to measure the amount of Gt bound to R\* before the addition of GTPγS. UM with Gt bound were resuspended in 10 mM Tris-HCl (pH 7.4), 0.5 mM MgCl<sub>2</sub>, 1 mM DTT, 0.1 mM PMSF, and 250 μM GTPγS, incubated on ice for 30 min, and centrifuged as described above. The supernatant and membrane-bound fractions were analyzed for the presence of G-protein subunits by immunoblotting. Quantification was by image analysis of the ECL films. Band intensity calculations were carried out in Image Gauge (FujiFilm).

## RESULTS

To study the involvement of individual amino acid side chains of the C-terminal region of Gtγ in interactions with light-activated rhodopsin, R\*, we have individually substituted each of 11 amino acid residues of the Gtγ(60–71) domain with alanine. The amino acid sequence of Gtγ and its alignment with other members of Gγ family are shown in Figure 1. Cysteine 71 was preserved in all mutants because it is the site of posttranslational farnesylation and carboxymethylation in native retinal rod cell Gtγ and is critical for Gt functions (13). Alanine is one of the most common natural amino acids and is the second-smallest amino acid after glycine. Unlike substitutions with glycine, alanine replacements are less likely to perturb the protein secondary structure, especially in α-helices (14). Because of these properties, alanine has been used historically in site-directed alanine scanning mutagenesis to replace the side chains under investigation with methyl group side chains.

Each Gtγ mutant was coexpressed with Gtβ-6-His in insect Sf9 cells using genetically engineered baculoviruses. Previous studies have shown that the baculovirus/insect cell system provides an excellent source of recombinant G-proteins, due to high levels of protein expression and the presence of intracellular machinery for effective posttranslational isoprenylation of G-protein γ subunits (5, 15–20).

To determine whether alanine replacements affected the membrane binding properties of the Gtβγ dimers, the aliquots of infected cells were lysed and the distribution of recom-

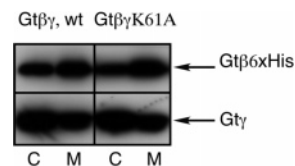


FIGURE 2: Interactions of Gtβγ with lipid membranes. Immunoblot of Gtβ (top) and Gtγ (bottom) in the cytosolic fraction (C) and the membrane fraction (M) of Sf9 cells after expression of the wild type (wt) and mutant Gtβγ. Identical results were obtained for all mutants. The data are representative of at least two independent experiments.

binant Gtβγ between the membrane and cytosolic fraction was compared to that of a wild-type recombinant Gtβγ. All mutants exhibited a distribution in the membrane and cytosol similar to that of wild-type Gtβγ (Figure 2). Only the membrane fraction, containing farnesylated Gtβγ, was used for further detergent extraction and purification on Ni-NTA affinity resin.

Affinity-purified recombinant Gtβγ dimers contained both Gtβ-6-His and mutant Gtγ in ratios identical to those of the wild-type Gtβγ dimers, which shows that none of the mutations affected the formation of the βγ complex. Protein concentrations were normalized between the various Gtβγ mutants by quantitative immunoblotting to ensure functional results can be compared directly. Purified recombinant Gtβ-6-His showed the expected increase in molecular mass of ~840 Da compared to the Gtβ purified from bovine retina rods (mass of 37 377 Da), due to the presence of a six-histidine tag at the N-terminus of the β subunit. This difference in molecular mass was helpful in distinguishing between binding of recombinant Gtβγ-6-His to rhodopsin membranes and the background level of native retinal Gtβγ always present in small amounts, even in urea-washed ROS membranes. Recombinant Gtγ mutants had a molecular mass similar to that of native Gtγ as determined from immunoblots of 12% Laemmli gels.

Transducin binds to light-activated rhodopsin in the absence of guanine nucleotide GTP or GDP to form a nucleotide-empty ternary R\*–Gt complex in the membrane. Addition of GTP, or nonhydrolyzable analogue GTPγS, activates transducin and dissociates the R\*–Gt complex. The amount of Gt bound and released by GTP can be visualized by gel staining or immunoblots. Originally developed by Kühn (21), the assay is based on the R\*–Gt binding and release which allows quantitative measurement of interactions of R\* with individual subunits of Gt (5, 7, 9, 16). Binding and GTP-induced release of Gtβγ from R\* are dependent on the presence of Gtα. No interactions of recombinant Gtβγ with R\* were observed when Gtα was omitted from the reaction mixture, which is evident from the lack of the higher-molecular mass band of Gtβ-6-His in GTPγS eluates even at high concentrations of the recombinant protein (Figure 3A).

To investigate the rhodopsin-interacting surface of the transducin γ subunit, and to evaluate how site-directed alanine replacements in the Gtγ(60–71) domain affect interactions with rhodopsin, equal amounts of recombinant Gtβγ mutants in identical dilution series were reconstituted with Gtα purified from bovine retinas and analyzed for interactions with R\*. GTPγS eluates were analyzed by quantitative immunoblotting for the presence of Gt, using a



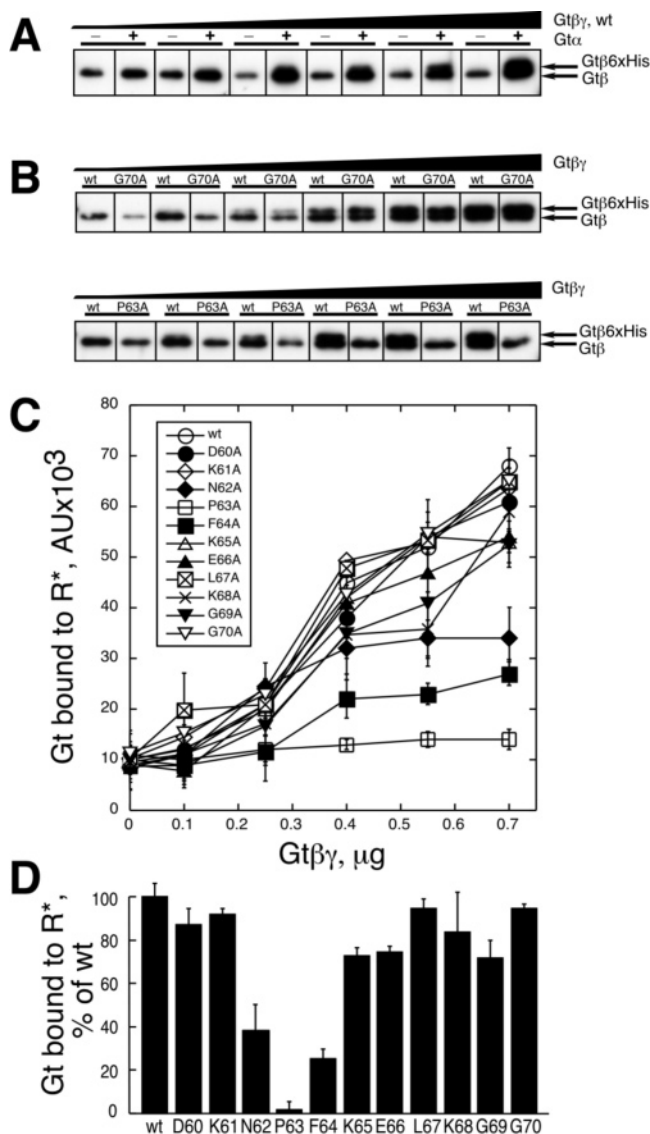


**FIGURE 3:** Interaction of  $Gt\beta\gamma$  mutants with light-activated rhodopsin in native membranes measured by binding and subsequent GTPγS-induced dissociation of the  $R^*$ –Gt complex. (A) The interaction of  $Gt\beta\gamma$  with  $R^*$  is  $Gt\alpha$  subunit-dependent. Increasing amounts of  $Gt\beta\gamma$  (0, 0.1, 0.25, 0.4, 0.55, and 0.7  $\mu$ g) from left to right are shown by the top bar. The absence and presence of 3  $\mu$ g of  $Gt\alpha$  for each dose of  $Gt\beta\gamma$  are indicated with minus and plus signs, respectively. The immunoblot of GTPγS eluates represents three independent experiments. (B) Western blot analysis of  $Gt\beta\gamma$ , wild type and mutants in pairs, in GTPγS eluates after interaction with the rhodopsin membranes in the presence of purified  $Gt\alpha$ . The bottom band ( $Gt\beta$ ) represents the background endogenous  $Gt\beta\gamma$  complex. The top band ( $Gt\beta\gamma$ -6-His) represents interactions of the recombinant  $Gt\beta\gamma$  (G70A or P63A) with rhodopsin under identical conditions. Starting amounts of the  $Gt\beta\gamma$  subunits were normalized in preliminary experiments. (C) Dose-dependent interaction of mutant  $Gt\beta\gamma$  with rhodopsin membranes, based on the quantitative densitometry of Western blots. The data represent two to five independent experiments for each mutant. (D) Maximal binding for individual mutants expressed in percentage points compared to the control, wild-type (wt)  $Gt\beta\gamma$ .

highly specific anti- $Gt\beta$  antibody (9), as shown for  $Gt\beta\gamma$  mutants G70A and P63A as examples (Figure 4B). For all mutants, the intensity of the recombinant  $Gt\beta$ -6-His band was quantified as shown in Figure 4C, and the maximal values were expressed in percentage points using interactions of wild-type (wt) Gt with  $R^*$  as 100% (Figure 4D). Four

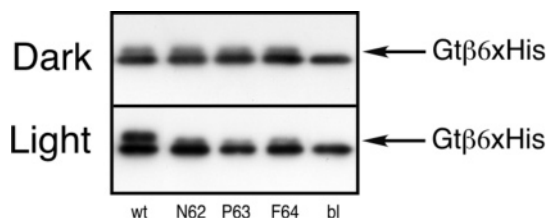


**FIGURE 4:**  $Gt\beta\gamma$  mutations affect formation of the  $R^*$ –Gt complex. Wild-type and mutant  $Gt\beta\gamma$  bound to dark-adapted (Dark) and light-activated (Light) rhodopsin membranes in the absence of nucleotides. The experimental conditions are as described in the legend of Figure 3 at 0.7  $\mu$ g of  $Gt\beta\gamma$ , 3  $\mu$ g of  $Gt\alpha$ , and 30  $\mu$ g of rhodopsin membranes. Blank reaction (bl) contained only rhodopsin membranes. The immunoblot represents two independent experiments.

mutants,  $Gt\beta\gamma$ D60A,  $Gt\beta\gamma$ K61A,  $Gt\beta\gamma$ L67A, and  $Gt\beta\gamma$ G70A, had activity almost identical to that of wild-type  $Gt\beta\gamma$ .  $Gt\beta\gamma$ K65A,  $Gt\beta\gamma$ E66A,  $Gt\beta\gamma$ K68A, and  $Gt\beta\gamma$ G69A mutations affected  $R^*$  interactions mildly, showing an activity that was  $\sim 70\%$  of that of the wild type.  $Gt\gamma$ P63A exhibited only residual activity compared to wild-type  $Gt\beta\gamma$ , while adjacent mutations  $Gt\gamma$ N62A and  $Gt\gamma$ F64A were at 38 and 25%, respectively. These functional defects can result from abnormalities at three different steps of the activation process: (1) binding of Gt to dark-adapted rhodopsin membranes, (2) formation of a nucleotide-free  $R^*$ –Gt complex, and (3) GTP-induced activation of  $Gt\alpha$  and dissociation of the complex. To discriminate between these possibilities, we reconstituted the three most affected  $Gt\beta\gamma$  mutants ( $Gt\gamma$ N62A, -P63A, and -F64A) with  $Gt\alpha$  and analyzed the amount of Gt bound to rhodopsin membranes in the dark, and after light activation in the absence of nucleotides. Binding to the dark rhodopsin membranes was identical for all mutants and the wild type (Figure 4). The amount of mutant Gt bound to light-activated rhodopsin membranes was affected significantly compared to that of the wild type (Figure 4). The results of light binding parallel well the results of GTPγS activation and complex dissociation (Figure 3D), strongly suggesting that the initial step of formation of the  $R^*$ –Gt complex is affected in all three mutants.

## DISCUSSION

Phototransduction in retinal rod cells is initiated by the interactions between photoactivated rhodopsin and the heterotrimeric transducin. In addition to the interactions between  $R^*$  and  $Gt\alpha$  leading to the nucleotide exchange,  $Gt\beta\gamma$  has been shown to play a pivotal allosteric role in supporting docking of the heterotrimer to  $R^*$  and facilitating  $Gt\alpha$  activation (22, 23). Early reports of direct interactions of  $Gt\beta\gamma$  with  $R^*$  (24–26) and the demonstration of an indispensable role of the farnesyl group in coupling with the activated receptor (13, 27) have been substantiated by the identification of the C-terminal domain on  $Gt\gamma$  involved in direct contacts with  $R^*$  (28).

The site of interactions with  $R^*$  on  $Gt\beta\gamma$  has been mapped to the  $Gt\gamma$ (60–71) region by peptide competition, peptide-induced extra Meta II, amino acid reversal mutagenesis, and NMR studies (5, 7, 28, 29). Experiments in two independent laboratories have shown recently that the C-terminal region of  $Gt\gamma$ , including the farnesyl group, undergoes significant conformational change upon interactions with  $R^*$  in native

lipid membranes (5–7). The changes include the movement of the farnesyl moiety and the reorganization of the Gt $\gamma$  C-terminal domain into an amphipathic helix. These results suggest strongly that the molecular surface on Gt $\beta\gamma$  presented for interactions with R\* is substantially different from the conformation observed in the X-ray structures of Gt $\beta\gamma$  (30).

It has specifically been proposed that the F64 side chain in Gt $\gamma$  changes orientation dramatically from facing Gt $\beta$  to facing R\* and that P63 immediately preceding the helix may serve as an anisotropic molecular hinge (5). This model, based on the NMR of a synthetic peptide, requires testing on the level of a holo-G-protein. We introduced alanine substitutions in 11 positions along the Gt $\gamma$ (60–70) stretch, coexpressed the recombinant proteins with Gt $\beta$  using the Sf9/baculovirus system, and purified the Gt $\beta\gamma$  dimers containing corresponding C-terminal mutations in Gt $\gamma$ . After reconstitution with pure retinal Gt $\alpha$ , holo-Gts with mutations N62A, P63A, and F64A were unable to interact with R\* effectively (Figure 3). Additional analysis revealed that while binding to the dark-adapted rhodopsin membranes was normal for these mutants, binding to R\* was significantly impaired (Figure 4). These results argue that N62A, P63A, and F64A mutations affect formation of the nucleotide-empty R\*–Gt complex, rather than the subsequent step of GTP-induced activation of Gt $\alpha$ . The location of functionally important N62, P63, and F64 at the N-terminus of Gt $\gamma$ (60–71) is consistent with metarhodopsin II stabilization by farnesylated peptides of varying sizes. The peptide data showed that inclusion of Gt $\gamma$ (62–64) is obligatory for interactions with Meta II, while the Gt $\gamma$ (65–71) region was necessary but insufficient for activity (31).

Four positions in Gt $\gamma$ , D60, K61, L67, and G70, tolerated replacements with alanine well, which suggests that these amino acids are not involved in R\* interactions. Previous mutational studies using synthetic peptides identified the F64–L67 region as being generally important for stabilization of Meta II (7). The data presented here narrow this region to the aromatic side chain of F64. The mechanism of inactivating mutations in the Gt(60–71) region by multiple mutations reported earlier can be more complex, however, through disruption of specific involvement of the F64 side chain in R\* interactions and also through structural interference in helix formation as has been shown for the K65E66 reversal mutant (5).

Several mutants, K65A, E66A, K68A, and G69A, exhibited only mild reduction in activity. Because the side chains of these amino acids do not appear to form a unified interface, the mechanism of these mutations is likely due to the partial negative effect on helix formation in this region during binding to R\*. Mutation of two adjacent glycine residues at the very C-terminus immediately before farnesylated C71 had a mixed effect on R\* coupling: the G69A mutant was partially active at ~70% of the level of the wild type, while G70A was fully active. The fact that G69A and G70A individually did not have a major effect on R\* interactions suggests that either the high mobility of the polypeptide chain in this region is not necessary for the conformational changes involving farnesyl group and helix formation or only one glycine is sufficient for ensuring high conformational mobility. Double mutant G69A/G70A may answer this question fully. Overall, it appears that the N-terminal portion of the C-terminal helical domain of Gt $\gamma$

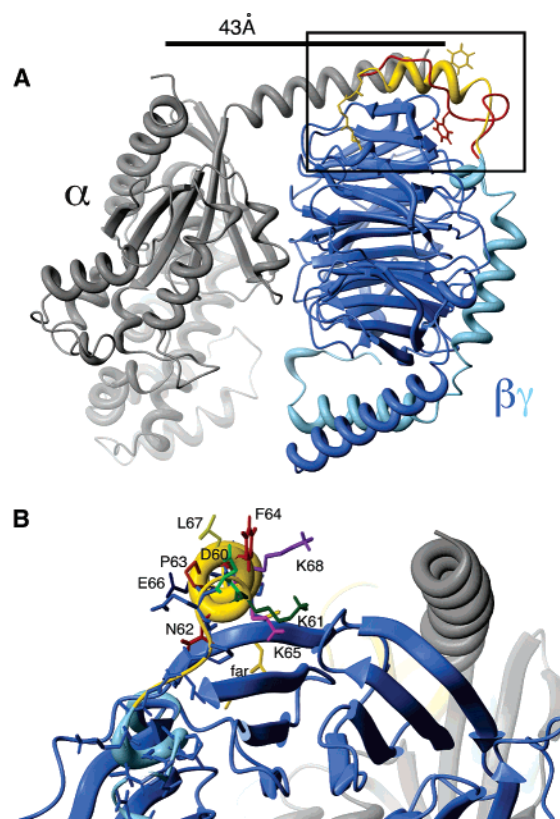


FIGURE 5: Ribbon diagram of Gt based on the X-ray crystallographic studies (PDB entry 1GOT). The conformations of Gt $\alpha$  (340–350) [PDB entry 1AQG (44)] and Gt $\gamma$ (60–71) [PDB entry 1MF6 (5)] are shown in the R\*-bound state. (A) The ground conformation of Gt $\gamma$ (60–71)farnesyl is colored red and the R\*-bound form yellow. The change in the position of F64 from facing the Gt $\beta$  to facing rhodopsin is highlighted. The distance between Gt $\alpha$  L349 and Gt $\gamma$  F64 is 43 Å. (B) Close-up of the inset in panel A, rotated horizontally by 90°. Residues affected most by alanine replacements, N62, P63, and F64, are colored red.

in the R\*-bound form is critically important for R\* interactions (Figure 5).

Amino acid residues N62, P63, and F64 are highly conserved among all members of the G $\gamma$  subunit family (Figure 1). Our results explain this conservation, as mutations at these positions lead to the reduced level of interaction with rhodopsin. The pattern of P63 conservation reveals an interesting observation.

P63 is highly conserved among all classes of mammalian G $\gamma$  subunits, from subtype 1 to 13 (Figure 1), and G $\gamma$ s found in *Caenorhabditis elegans* and *Drosophila melanogaster*. Interestingly, G $\gamma$  subunits involved in pheromone responses in budding yeast are exceptions to this rule. This unique feature of yeast G $\gamma$  may explain a report that the G $\gamma$  tail is dispensable in pheromone signaling (32), although the contribution of other factors, such as the much larger length of the yeast G $\gamma$  C-terminal domain, cannot be ruled out (mammalian G $\gamma$  domains have seven amino acids between P63 and C71 of the CAAX box, while the corresponding domain in yeast is 21 amino acids long). It is also possible that pheromone signaling in budding yeast relies on the evolutionarily earlier and simpler GPCR/G-protein system.

Of special interest for the mechanism of Gt activation is the observation that mutations that affect R\* binding the most are located on the outer edge of Gt $\gamma$  that is farther from the Gt $\alpha$  subunit. The distance between amino acid side chains



that have been shown to be critical for R\* binding, Gt $\alpha$  L349 and Gt $\gamma$  F64, is 43 Å (Figure 5B). The rhodopsin cytoplasmic surface in the inactive dark state is elliptical with physical side-to-side dimensions of 45 Å for a major axis and 27 Å for a minor axis. The more realistic functionally important area is only ~30 Å in diameter, which encompasses loop 2, loop 3, and the N-terminus of helix 8. Numerous studies have shown that upon light activation the cytoplasmic surface increases in size by up to 8 Å, in response to the outward movements of transmembrane helices, most notably helix 6 (TM6) (33–35). The model of the Meta II state built on the basis of these experimental data has taken into account energetically favorable modes of conformational changes and inherent flexibility of the cytoplasmic loops (36, 37). It reveals that light activation increases the size of the minor axis to approximately 31–33 Å. It is clear that the distance of 43 Å between the two Gt domains is too large for simultaneous interaction with the R\* monomer, as predicted in a 1:1 model of the R\*–Gt complex (38).

Three potential scenarios may help to reconcile this discrepancy. (1) A significant change in tilt between subunits, bringing the C-termini of Gt $\alpha$  and Gt $\gamma$  closer together (39), has been proposed. The lever hypothesis provides a compelling way for R\* to exert an allosteric effect on the nucleotide-binding site via Gt $\beta\gamma$  contacts with switch regions II and III on Gt $\alpha$  (39). (2) Interaction of a single Gt with a rhodopsin dimer has strong support from the atomic microscopy experiments (40). This hypothesis does not call for a large reorganization of the Gt subunit interface, thus satisfying the current paradox between the small diameter of the rhodopsin monomer and the large footprint from R\* on Gt. The dimer hypothesis does not explain at present, however, the fact that both C-terminal domains of Gt can interact only with active Meta II and not inactive dark-adapted rhodopsin. Both rhodopsin units in a dimer must be light-activated to interact with the C-termini of Gt $\alpha$  and Gt $\gamma$ . This requirement clashes with the known property of the phototransduction pathway which is to be activated by a single photon of light (41). (3) The third mechanism, R\*–Gt coupling via two-site sequential fit interactions, has also been proposed (29, 42, 43). This mechanism suggests temporal separation of interactions between Gt $\alpha$ –R\* and Gt $\gamma$ –R\* complexes, with each step having a discrete structural impact on Gt, and possibly on R\* conformations, ultimately leading to nucleotide release. Further experiments are required to discriminate among the three mechanisms.

In conclusion, using site-directed alanine scanning mutagenesis of the C-terminal region of Gt $\gamma$ , we mapped the location of a conserved regulatory switch involved in R\*–Gt interactions. Disabling of this switch, which includes amino acids N62, P63, and F64, significantly impairs Gt activation by weakening the ability of mutant Gt to form a complex with light-activated rhodopsin. The location of N62, P63, and F64 at the N-terminal part of an amphipathic helix formed during binding to R\* places important distance constraints on the R\*–Gt complex.

## ACKNOWLEDGMENT

We thank Dr. N. Gautam for support and discussions.

## REFERENCES

- Arshavsky, V. Y., Lamb, T. D., and Pugh, E. N., Jr. (2002) G proteins and phototransduction, *Annu. Rev. Physiol.* 64, 153–87.
- Hamm, H. E. (2001) How activated receptors couple to G proteins, *Proc. Natl. Acad. Sci. U.S.A.* 98, 4819–21.
- Helmreich, E. J., and Hofmann, K. P. (1996) Structure and function of proteins in G-protein-coupled signal transfer, *Biochim. Biophys. Acta* 1286, 285–322.
- Gautam, N., Downes, G. B., Yan, K., and Kisselev, O. (1998) The G-protein  $\beta\gamma$  complex, *Cell. Signalling* 10, 447–55.
- Kisselev, O. G., and Downs, M. A. (2003) Rhodopsin controls a conformational switch on the transducin gamma subunit, *Structure* 11, 367–73.
- Hagiwara, K., Wada, A., Katada, M., Ito, M., Ohya, Y., Casey, P. J., and Fukada, Y. (2004) Analysis of the molecular interaction of the farnesyl moiety of transducin through the use of a photoreactive farnesyl analogue, *Biochemistry* 43, 300–9.
- Kisselev, O., Pronin, A., Ermolaeva, M., and Gautam, N. (1995) Receptor-G protein coupling is established by a potential conformational switch in the  $\beta\gamma$  complex, *Proc. Natl. Acad. Sci. U.S.A.* 92, 9102–6.
- Kozasa, T. (2004) Purification of G protein subunits from Sf9 insect cells using hexahistidine-tagged  $\alpha$  and  $\beta\gamma$  subunits, *Methods Mol. Biol.* 237, 21–38.
- Kisselev, O. G., Pronin, A. P., and Gautam, N. (1999) in *G-proteins: Techniques of Analysis* (Manning, D. R., Ed.) pp 85–95, CRC Press, Boca Raton, FL.
- Wray, W., Boulukas, T., Wray, V. P., and Hancock, R. (1981) Silver staining of proteins in polyacrylamide gels, *Anal. Biochem.* 118, 197–203.
- Yamazaki, A., Yamazaki, M., Tsuboi, S., Kishigami, A., Umberger, K. O., Hutson, L. D., Madland, W. T., and Hayashi, F. (1993) Regulation of G protein function by an effector in GTP-dependent signal transduction. An inhibitory subunit of cGMP phosphodiesterase inhibits GTP hydrolysis by transducin in vertebrate rod photoreceptors, *J. Biol. Chem.* 268, 8899–907.
- Willardson, B. M., Pou, B., Yoshida, T., and Bitensky, M. W. (1993) Cooperative binding of the retinal rod G-protein, transducin, to light-activated rhodopsin, *J. Biol. Chem.* 268, 6371–82.
- Fukada, Y., Takao, T., Ohguro, H., Yoshizawa, T., Akino, T., and Shimonishi, Y. (1990) Farnesylated  $\gamma$ -subunit of photoreceptor G protein indispensable for GTP binding, *Nature* 346, 658–60.
- Lyu, P. C., Liff, M. I., Marky, L. A., and Kallenbach, N. R. (1990) Side chain contributions to the stability of  $\alpha$ -helical structure in peptides, *Science* 250, 669–73.
- Kozasa, T., Hepler, J. R., Smrcka, A. V., Simon, M. I., Rhee, S. G., Sternweis, P. C., and Gilman, A. G. (1993) Purification and characterization of recombinant G16 $\alpha$  from Sf9 cells: Activation of purified phospholipase C isozymes by G-protein  $\alpha$  subunits, *Proc. Natl. Acad. Sci. U.S.A.* 90, 9176–80.
- Kisselev, O., and Gautam, N. (1993) Specific interaction with rhodopsin is dependent on the  $\gamma$  subunit type in a G protein, *J. Biol. Chem.* 268, 24519–22.
- Fogg, V. C., Azpiazu, I., Linder, M. E., Smrcka, A., Scarlata, S., and Gautam, N. (2001) Role of the  $\gamma$  subunit prenyl moiety in G protein  $\beta\gamma$  complex interaction with phospholipase C $\beta$ , *J. Biol. Chem.* 276, 41797–802.
- Panchenko, M. P., Saxena, K., Li, Y., Charnecki, S., Sternweis, P. M., Smith, T. F., Gilman, A. G., Kozasa, T., and Neer, E. J. (1998) Sites important for PLC $\beta$ 2 activation by the G protein  $\beta\gamma$  subunit map to the sides of the  $\beta$  propeller structure, *J. Biol. Chem.* 273, 28298–304.
- Wickman, K. D., Iniguez-Lluhl, J. A., Davenport, P. A., Taussig, R., Krapivinsky, G. B., Linder, M. E., Gilman, A. G., and Clapham, D. E. (1994) Recombinant G-protein  $\beta\gamma$ -subunits activate the muscarinic-gated atrial potassium channel, *Nature* 368, 255–7.
- Myung, C. S., Yasuda, H., Liu, W. W., Harden, T. K., and Garrison, J. C. (1999) Role of isoprenoid lipids on the heterotrimeric G protein  $\gamma$  subunit in determining effector activation, *J. Biol. Chem.* 274, 16595–603.
- Kühn, H. (1984) *Interactions between photoexcited rhodopsin and light-activated enzymes in rods*, Vol. 3, Pergamon Press, Oxford, U.K.
- Kühn, H. (1980) Light- and GTP-regulated interaction of GTPase and other proteins with bovine photoreceptor membranes, *Nature* 283, 587–9.
- Fung, B. K., Hurley, J. B., and Stryer, L. (1981) Flow of information in the light-triggered cyclic nucleotide cascade of vision, *Proc. Natl. Acad. Sci. U.S.A.* 78, 152–6.

24. Kelleher, D. J., and Johnson, G. L. (1988) Transducin inhibition of light-dependent rhodopsin phosphorylation: Evidence for  $\beta\gamma$  subunit interaction with rhodopsin, *Mol. Pharmacol.* **34**, 452–60.
25. Phillips, W. J., and Cerione, R. A. (1992) Rhodopsin/transducin interactions. I. Characterization of the binding of the transducin- $\beta\gamma$  subunit complex to rhodopsin using fluorescence spectroscopy, *J. Biol. Chem.* **267**, 17032–9.
26. Halpern, J. L., Chang, P. P., Tsai, S. C., Adamik, R., Kanaho, Y., Sohn, R., Moss, J., and Vaughan, M. (1987) Production of antibodies against rhodopsin after immunization with  $\beta\gamma$ -subunits of transducin: Evidence for interaction of  $\beta\gamma$ -subunits of guanosine 5'-triphosphate binding proteins with receptor, *Biochemistry* **26**, 1655–8.
27. Ohguro, H., Fukada, Y., Takao, T., Shimonishi, Y., Yoshizawa, T., and Akino, T. (1991) Carboxyl methylation and farnesylation of transducin  $\gamma$ -subunit synergistically enhance its coupling with metarhodopsin II, *EMBO J.* **10**, 3669–74.
28. Kisselev, O. G., Ermolaeva, M. V., and Gautam, N. (1994) A farnesylated domain in the G protein  $\gamma$  subunit is a specific determinant of receptor coupling, *J. Biol. Chem.* **269**, 21399–402.
29. Kisselev, O. G., Meyer, C. K., Heck, M., Ernst, O. P., and Hofmann, K. P. (1999) Signal transfer from rhodopsin to the G-protein: Evidence for a two-site sequential fit mechanism, *Proc. Natl. Acad. Sci. U.S.A.* **96**, 4898–903.
30. Sondek, J., Bohm, A., Lambright, D. G., Hamm, H. E., and Sigler, P. B. (1996) Crystal structure of a G $\alpha$  protein  $\beta\gamma$  dimer at 2.1 Å resolution, *Nature* **379**, 369–74.
31. Kisselev, O. G., Ermolaeva, M. V., and Gautam, N. (1995) Efficient interaction with a receptor requires a specific type of prenyl group on the G protein  $\gamma$  subunit, *J. Biol. Chem.* **270**, 25356–8.
32. Chinault, S. L., and Blumer, K. J. (2003) The C-terminal tail preceding the CAAX box of a yeast G protein  $\gamma$  subunit is dispensable for receptor-mediated G protein activation in vivo, *J. Biol. Chem.* **278**, 20638–44.
33. Hubbell, W. L., Altenbach, C., Hubbell, C. M., and Khorana, H. G. (2003) Rhodopsin structure, dynamics, and activation: A perspective from crystallography, site-directed spin labeling, sulfhydryl reactivity, and disulfide cross-linking, *Adv. Protein Chem.* **63**, 243–90.
34. Sakmar, T. P., Menon, S. T., Marin, E. P., and Awad, E. S. (2002) Rhodopsin: Insights from recent structural studies, *Annu. Rev. Biophys. Biomol. Struct.* **31**, 443–84.
35. Okada, T., Ernst, O. P., Palczewski, K., and Hofmann, K. P. (2001) Activation of rhodopsin: New insights from structural and biochemical studies, *Trends Biochem. Sci.* **26**, 318–24.
36. Nikiforovich, G. V., and Marshall, G. R. (2003) Three-dimensional model for meta-II rhodopsin, an activated G-protein-coupled receptor, *Biochemistry* **42**, 9110–20.
37. Nikiforovich, G. V., and Marshall, G. R. (2005) Modeling flexible loops in the dark-adapted and activated states of rhodopsin, a prototypical G-protein-coupled receptor, *Biophys. J.* **89**, 3780–9.
38. Chabre, M., and le Maire, M. (2005) Monomeric G-protein-coupled receptor as a functional unit, *Biochemistry* **44**, 9395–403.
39. Rondard, P., Iiri, T., Srinivasan, S., Meng, E., Fujita, T., and Bourne, H. R. (2001) Mutant G protein  $\alpha$  subunit activated by G $\beta\gamma$ : A model for receptor activation? *Proc. Natl. Acad. Sci. U.S.A.* **98**, 6150–5.
40. Fotiadis, D., Liang, Y., Filipek, S., Saperstein, D. A., Engel, A., and Palczewski, K. (2003) Atomic-force microscopy: Rhodopsin dimers in native disc membranes, *Nature* **421**, 127–8.
41. Baylor, D. A., Lamb, T. D., and Yau, K. W. (1979) Responses of retinal rods to single photons, *J. Physiol.* **288**, 613–34.
42. Herrmann, R., Heck, M., Henklein, P., Kleuss, C., Hofmann, K. P., and Ernst, O. P. (2004) Sequence of interactions in receptor-G protein coupling, *J. Biol. Chem.* **279**, 24283–90.
43. Nanoff, C., Koppensteiner, R., Yang, Q., Fuerst, E., Ahorn, H., and Freissmuth, M. (2006) The carboxyl terminus of the G $\alpha$ -subunit is the latch for triggered activation of heterotrimeric G proteins, *Mol. Pharmacol.* **69**, 397–405.
44. Kisselev, O. G., Kao, J., Ponder, J. W., Fann, Y. C., Gautam, N., and Marshall, G. R. (1998) Light-activated rhodopsin induces structural binding motif in G protein  $\alpha$  subunit, *Proc. Natl. Acad. Sci. U.S.A.* **95**, 4270–5.

BI060806X